# Proteomic Analysis of Mammalian Oligosaccharyltransferase Reveals Multiple Subcomplexes that Contain Sec61, TRAP, and Two Potential New Subunits†

Toru Shibatani,‡ Larry L. David,§ Ashley L. McCormack,|| Klaus Frueh,|| and William R. Skach*,‡

*Division of Molecular Medicine, Oregon Health and Sciences University, 3181 Southwest Sam Jackson Park Road, Portland, Oregon 97201, School of Dentistry, Oregon Health and Sciences University, 611 Southwest Campus Drive, Portland, Oregon 97239-3098, and Oregon National Primate Research Center, Oregon Health and Sciences University, 505 Northwest 185th Avenue, Beaverton, Oregon 97006-3448*

*Received December 20, 2004; Revised Manuscript Received March 1, 2005*

ABSTRACT: Oligosaccharyltransferase (OST) catalyzes the cotranslational transfer of high-mannose sugars to nascent polypeptides during N-linked glycosylation in the rough endoplasmic reticulum lumen. Nine OST subunits have been identified in yeast. However, the composition and organization of mammalian OST remain unclear. Using two-dimensional Blue Native polyacrylamide gel electrophoresis/sodium dodecyl sulfate−polyacrylamide gel electrophoresis and mass spectrometry, we now demonstrate that mammalian OST can be isolated from solubilized, actively engaged ribosomes as multiple distinct protein complexes that range in size from ∼500 to 700 kDa. These complexes exhibit different ribosome affinities and subunit compositions. The major complex, $OSTC_I$, had an apparent size of ∼500 kDa and was readily released from ribosome translocon complexes after puromycin treatment under physiological salt conditions. Two additional complexes were released only after treatment with high salt: $OSTC_{II}$ (∼600 kDa) and $OSTC_{III}$ (∼700 kDa). Both remained stably associated with heterotrimeric Sec61$\alpha\beta\gamma$, while $OSTC_{III}$ also contained the tetrameric TRAP complex. All known mammalian OST subunits (STT3-A, ribophorin I, ribophorin II, OST48, and DAD1) were present in all complexes. In addition, two previously uncharacterized proteins were also copurified with OST. Mass spectrometry identified a 17 kDa protein as DC2 which is weakly homologous to the C-terminal half of yeast Ost3p and Ost6p. The second protein (14 kDa) was tentatively identified as keratinocyte-associated protein 2 (KCP2) and has no previously known function. Our results identify two potential new subunits of mammalian OST and demonstrate a remarkable heterogeneity in OST composition that may reflect a means for controlling nascent chain glycosylation.

During translocation into the endoplasmic reticulum (ER),[1] nascent polypeptides are covalently modified by an attachment of high-mannose core oligosaccharides at consensus Asn-X-Ser/Thr sequons (*1*). These N-linked carbohydrates play key roles in facilitating interactions with ER chaperones such as calnexin and calreticulin, and thus help to ensure correct folding of newly synthesized proteins (*2*−*4*). N-Linked glycosylation is carried out by a large protein complex, oligosaccharyltransferase (OST) or oligosaccharyl transferase (OT) (*5*−*9*). In the yeast *Saccharomyces cerevisiae*, OST contains at least eight separate subunits, five of which are essential for viability, Stt3p, WbpI, Swp1, Ost1p (also known as Nlt1p), and Ost2p (*5*, *10*−*15*). Two highly homologous proteins, Ost3p and Ost6p, are nonessential but facilitate glycosylation of specific substrates (*16*, *17*). Ost4p and Ost5p are also nonessential and are required for optimal OST activity (*18*, *19*).

Five subunits have been identified in mammalian OST and correspond to their yeast homologues, STT3-A/B (Stt3p), ribophorin I (Ost1p), ribophorin II (Swp1p), OST48 (Wbp1p), and DADI (Ost2p) (*7*, *20*−*22*). Among the mammalian subunits, ribophorin II is unique in that its molecular size (63 kDa) is twice that of its yeast counterpart. A potential mammalian homologue of yeast Ost4p has also been identified for human and mouse on the basis of sequence homology (*23*), although its association with mammalian OST has not yet been reported. Recently, OST complexes have been isolated from canine pancreatic ER membranes that contain different STT3 isoforms (STT3-A and STT3-B). These complexes exhibit different enzymatic activities, suggesting that nascent chain glycosylation can be regulated at the level of STT3 subunit association (*20*). Two possible mammalian homologues of Ost3p and Ost6p, N33 and IAP, have also been proposed on the basis of sequence homology and predicted oxidoreductase activity (*17*, *20*, *24*). N33 has been shown to comigrate with solublized OST activity on glycerol gradients, but neither protein has yet been isolated in association with purified OST complexes (*20*).

† This work was supported by NIH Grant GM53457 (W.R.S.), Grant DK51818 (W.R.S.), Core Grant EY10572, and Grant T32HL07781 (T.S.) and by Cystic Fibrosis Foundation Therapeutics Inc. (W.R.S.).

* To whom correspondence should be addressed: Division of Molecular Medicine, Oregon Health and Sciences University, 3181 SW Sam Jackson Park Rd., Portland, OR 97239. Phone: (503) 494-7322. Fax: (503) 494-7368. E-mail: skachw@ohsu.edu.

‡ Division of Molecular Medicine.

§ School of Dentistry.

|| Oregon National Primate Research Center.

[1] Abbreviations: BN-PAGE, Blue Native polyacrylamide gel electrophoresis; DTT, dithiothreitol; ER, endoplasmic reticulum; EST, expressed sequence tags; KCP2, keratinocyte-associated protein 2; OST, oligosaccharyltransferase; OT, oligosaccharyl transferase; M-V, mitochondrial respiratory complex V; RAMP, ribosome-associated membrane protein; RTC, ribosome−translocon complex; SPC, signal peptidase complex; TRAM, translocating chain-associating membrane protein; TRAP, translocation-associated protein.

10.1021/bi047328f CCC: $30.25 
Published on Web 04/02/2005

For most glycoproteins, N-linked glycosylation occurs cotranslationally as the nascent polypeptide emerges from the translocon into the ER lumen (*25*), and glycosylation efficiency increases significantly when the consensus site extends more than 12−14 residues from the ER membrane (*26*, *27*). Recent cross-linking studies have also demonstrated that the Asn consensus site interacts with the STT3-A subunit when it extends approximately 65−75 residues from the ribosome peptidyl transferase center (*28*). Thus, OST is thought to comprise a peripheral component of ER translocation machinery that continuously scans polypeptides for the presence of potential glycosylation sites. Consistent with this, ribophorin I and II have been copurified with actively engaged ribosomes isolated from native ER membranes under mild detergent conditions (*29*−*31*) and therefore constitute components of the ribosome-associated membrane protein (RAMP) fraction. The RAMP fraction also contains proteins directly involved in translocation that include the Sec61α$\beta\gamma$ heterotrimer and the translocation-associated protein TRAP (α, $\beta$, $\gamma$, and $\delta$ subunits) (*29*, *31*, *32*). However, despite evidence that OST is adjacent to the ER Sec61 translocon (*30*, *33*), little is known about whether it interacts directly with other RAMP proteins and how it is localized to actively translating ribosomes at the ER membrane.

In this study, we have used Blue Native polyacrylamide gel electrophoresis (BN-PAGE) to examine the organization and subunit composition of mammalian OST bound to actively engaged ribosome translocon complexes (RTCs). This technique enables isolation and separation of large membrane protein complexes with minimal perturbation of native composition using Coomassie G250 dyes as the charged ion carrier. BN-PAGE has been widely used in the study of respiratory chain complexes from the inner mitochondrial membrane (*34*, *35*). It also provides a powerful approach for isolating and purifying solubilized RAMP complexes from ER because ribosome−translocon interactions are dependent on the presence of a nascent translocating polypeptide which can be released by the aminoacyl-tRNA analogue puromycin (*31*). Here we have exploited this approach in conjunction with mass spectrometry to characterize the size and subunit composition of OST released from engaged RTCs. We now demonstrate that mammalian OST can be isolated in at least three stable complexes with sizes ranging from ∼500 to ∼700 kDa. The largest of these represent supercomplexes that are tightly bound to ribosomes even after nascent polypeptide release and retain stable associations with the Sec61α$\beta\gamma$ complex and TRAPα$\beta\gamma\delta$ complex after dissociation from the ribosome. We also found two new proteins that copurified with mammalian OST. The first is a 17 kDa protein, identified as DC2, which is weakly homologous to the C-terminal domain of yeast Ost3p and Ost6p. The second is a novel 14 kDa protein of unknown function. These two proteins were present in all three OST complexes. The heterogeneous composition of OST on engaged RTCs demonstrates that OST can form stable supercomplexes with ER translocon components, and raises the possibility that higher-order structures may represent different stages of translocon engagement during nascent chain N-linked glycosylation.

## MATERIALS AND METHODS

*Isolation of RAMP Proteins.* Rough microsomes were prepared from canine pancreas (*36*, *37*), and the RAMP fraction was isolated as described by Wang and Dobberstein (*31*) with the following modifications. Microsomes were solubilized and adjusted to a concentration of 0.25 equiv/$\mu$L [1 equiv = 1 $\mu$L of solubilized microsomal membranes with an $OD_{280}$ of 50 (*36*)] with 2% digitonin (CalBiochem, San Diego, CA) and 150 or 300 mM NaCl in S buffer [20 mM Tris-HCl (pH 7.6), 5 mM $MgOAc_2$, 2 mM DTT, 12% (w/v) glycerol, and Protein Inhibitor III (CalBiochem)]. Samples were centrifuged at 10000*g* for 10 min at 4 °C to remove insoluble materials, and the supernatant was then centrifuged at 350000*g* for 60 min to pellet ribosome−translocon complexes. The resultant supernatant (pre-RAMP) was removed. Pellets were resuspended in 2 mM puromycin, 2 mM GTP, and 150 or 1000 mM NaCl in buffer A [100 mM HEPES-NaOH (pH 7.8), 15 mM $MgOAc_2$, 5 mM DTT, Protein Inhibitor III, 15% (w/v) glycerol, and 1% digitonin] and incubated at 24 °C for 1 h to release nascent chains and RAMPs from ribosomes. The reaction mixture was centrifuged at 350000*g* for 90 min to repellet ribosomes. Supernatants containing the RAMP fractions were removed and subjected to BN-PAGE.

For differential release of OST complexes, pellets from the first 350000*g* centrifugation were washed three times with 150 mM NaCl in buffer A and centrifuged at 350000*g* for 90 min to remove loosely associated RAMP proteins prior to incubation in 2 mM puromycin, 2 mM GTP, and 150 mM NaCl in buffer A at 24 °C for 1 h. Ribosomes were then washed once more with the same buffer and pelleted by centrifugation at 350000*g* for 90 min. The resultant pellet was then resuspended with puromycin, GTP, and 1000 mM NaCl in buffer A to strip tightly bound RAMP proteins from ribosomes. The sample was then centrifuged at 350000*g* for 90 min. This supernatant was designated as the post-RAMP fraction as shown in Figure 1.

*Blue Native Polyacrylamide Gel Electrophoresis and Two-Dimensional SDS−PAGE.* RAMP proteins were subjected to BN-PAGE based on the protocol described by Schägger and von Jagow (*31*, *34*, *35*) as follows. BN-PAGE gels were cast as a 6 to 13% gradient in 50 mM BisTris-HCl (pH 7.0) and 500 mM aminocaproic acid and overlaid with a 4% stacking gel. The RAMP fraction was mixed with $^1/_{40}$ volume of gel loading buffer [5% Serva Blue G in 500 mM aminocaproic acid (pH 7.0)] just before electrophoresis. For one-dimensional BN-PAGE, the total RAMP protein derived from 7 equiv of microsomal membranes was loaded per well, whereas for two-dimensional (2D) analysis, protein derived from 21 equiv of microsomal membranes was loaded per well. Thyroglobulin (670 kDa), ferritin (440 kDa), and bovine serum albumin (dimer, 133 kDa; and monomer, 66 kDa) were used as molecular mass markers. Gels were run in a cold room (4 °C) at 65 V for 16 h with cathode buffer [50 mM Tricine, 15 mM BisTris (pH 7.0), and 0.02% Serva Blue G] and anode buffer [50 mM BisTris-HCl (pH 7.0)]. Cathode buffer was then changed to contain 0.002% Serva Blue G dye (to aid in protein visualization), and electrophoresis was continued at 500 V until the dye front reached the end of the gel. For 2D analysis, individual lanes lane were excised, incubated in 1% DTT in 62.5 mM Tris-HCl

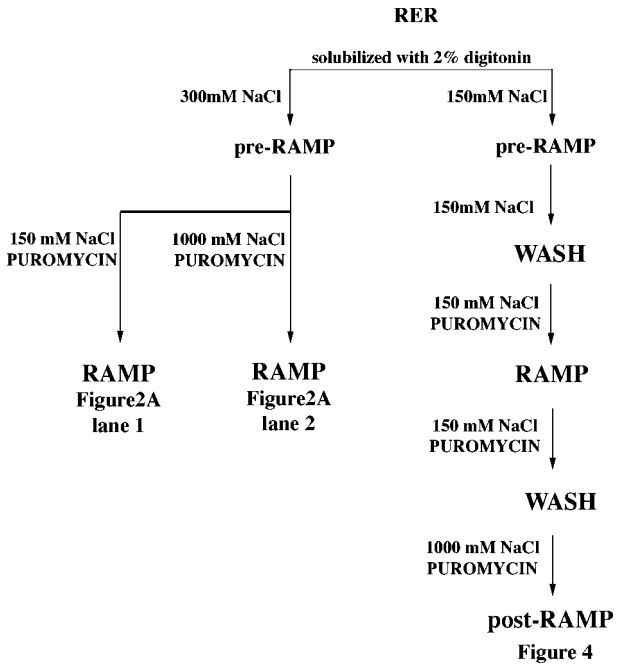


FIGURE 1: Strategy for RAMP preparation. Canine pancreatic rough ER microsomes (RER) were used for the isolation of the RAMP fraction. The salt concentrations during digitonin solubilization and puromycin release are indicated along each arrow. The pre-RAMP fraction designates the first supernatant after the first ultracentrifugation. The WASH fraction indicates the repeated resuspension and pelleting of RTCs under the conditions that are indicated. RAMP fractions represent the supernatant after puromycin treatment and ultracentrifugation. The post-RAMP fraction is the ultracentrifugation supernatant obtained by puromycin and high-salt treatment of puromycin-released RTCs.

(pH 6.8), 10% (w/v) glycerol, and 2% SDS for 20 min at 24 °C, and alkylated with 2.5% iodoacetamide in 62.5 mM Tris-HCl (pH 6.8), 10% glycerol, and 2% SDS for 20 min at 24 °C. The treated gel strip was subjected to SDS−PAGE using a 4% stacking gel and a 12 to 17% gradient gel as described by Laemmli (*38*). Gels were silver-stained according to modified Blum method (*39*, *40*). The gel was fixed with 40% (v/v) ethanol and 10% (v/v) acetic acid, washed thrice with 30% ethanol for 20 min, and washed once with $ddH_2O$. The gel was sensitized with 0.02% sodium thiosulfate followed by washing three times with $ddH_2O$. The gel was then incubated with 0.1% silver nitrate for 20 min at 4 °C, rinsed three times, and developed with 3% sodium carbonate and 0.05% formalin. All gels were scanned using a Umax Power Look III transmission scanner (Lexmark, Dallas, TX), and images were processed using Adobe Photoshop.

*Proteolytic Digestion.* Proteins were trypsin-digested in situ as described elsewhere (*41*, *42*). Silver-stained gel bands were excised, dried, and destained by incubation in 15 mM potassium ferricyanide and 50 mM sodium thiosulfate at 24 °C for 15 min, and then washed with 100 mM ammonium bicarbonate. Destained gels were dried and rehydrated with 0.01 mg/mL sequence-grade modified porcine trypsin (Promega, Madison, WI) in 50 mM ammonium bicarbonate and 5 mM $CaCl_2$ and incubated at 37 °C overnight. Trypsinized fragments were collected by sonicating gel pieces in 50 $\mu$L of 25 mM ammonium biocarbonate and again after adding 50 $\mu$L of 50% acetonitrile. The supernatant was collected and sonicated repeatedly in 50 $\mu$L of 5% formic acid and again after adding 50 $\mu$L of 50% acetonitrile. The supernatants were pooled; DTT was added to a final concentration of 1 mM, and the sample was dried and frozen at −80 °C for MS/MS.

*Tandem Mass Spectrometry.* The dried samples were dissolved in 10−20 mL of 5% formic acid and analyzed by liquid chromatography−electrospray ionization tandem mass spectrometry (LC−MS/MS) using either an LCQ Classic ion trap mass spectrometer (ThermoFinnigan, San Jose, CA) or an LCQ Deca XP Plus ion trap mass spectrometer (ThermoFinnigan).

LC−MS/MS using the LCQ Classic mass spectrometer utilized a 10 cm × 75 $\mu$m capillary column (15 $\mu$m tip PicoFrit, New Objectives, Woburn, MA), packed with 5 mm Zorbax SB-C18 material (Agilent Technologies, Wilmington, DE). Samples were applied to the column via a capillary trapping cartridge (Michrom Bioresources Inc., Auburn, CA), and peptides were separated using a 200 nL/min flow rate, a mobile phase containing 0.2% acetic acid, 0.005% heptafluorobutyric acid, and a 60 min 0 to 30% acetonitrile gradient. Peptide analysis using the LCQ Deca XP Plus mass spectrometer utilized a 10 cm × 180 $\mu$m capillary column packed with Biobasic-C18 (Thermo Hypersil Keystone, West Palm Beach, FL). Samples were applied to the column directly from the Finnigan Surveyor autosampler (ThermoElectron, San Jose, CA) using a Finnigan Surveyor sample pump (ThermoElectron) at a flow rate of 1 $\mu$L/min. The peptides were eluted from the column using a mobile phase of 0.1% formic acid in water and a 30 min 0 to 50% acetonitrile gradient. Peptide ions were analyzed using data-dependent scanning. Both instruments were set to trigger data-dependent MS/MS acquisition of the three most intense ions detected during the MS survey scan.

Tandem mass spectra were analyzed using the Sequest algorithm (ThermoFinnigan) as described by Eng and co-workers (*43*) using both the nonredundant protein database downloaded from the National Center for Biotechnology Information (NCBI) website (http://www.ncbi.nlm.nih.gov/, accessed Sept 1, 2004) and the Swiss-Prot protein database (Release 43, http://www.us.expasy.org/, accessed June 7, 2004). The search results derived from the NCBI protein database were subsequently filtered using DTAselect as described by Tabb et al. (*44*). Score thresholds were used (+1 ions, Xcorr > 1.7; +2 ions, Xcorr > 2.5; +3 ions, Xcorr > 3.5 and DelCn > 0.08 for all charge states), and all results were manually inspected.

Tandem mass spectra were also analyzed using the Opensea (version 1.2.2) alignment algorithm in conjunction with the de novo sequencing software Lutefisk (LutefiskXP version 1.0) (*45*) as described by Searle and co-workers (*46*, *47*). Spectra files were analyzed using the default ion trap parameters for LutefiskXP, including a peptide molecular weight tolerance of 0.5 and a fragment ion tolerance of 0.4. The protein databases (Swiss-Prot and NCBI) were automatically searched with the LutefiskXP-derived de novo sequences using the default Opensea parameters with a minimum protein score of 1.0. All results were manually inspected.

Protein fragments and sequences identified by mass spectrometry were further analyzed by a BLAST search against all nonredundant GenBank protein sequences (*48*). The Conserved Domain Database (CDD, NCBI) was utilized

to compare novel sequences with the known domain architecture database (*49*). To analyze the presence of signal sequence and transmembrane domains, Simple Modular Architecture Research Tool (SMART, http://smart.embl-heidelberg.de/) was also utilized (*50*, *51*). Hydropathy was examined using Kyte−Doolittle plots (*52*).

*Western Blotting.* Membrane proteins separated by 2D PAGE were transferred to the polyvinylidene fluoride (PVDF) membranes (Bio-Rad, Hercules, CA) using a Western blotting transfer unit and a Trans-Blot SD Semi-Dry Transfer Cell (Bio-Rad) at 20 V for 1 h using Towbin buffer [25 mM Tris-HCl (pH 7.4), 192 mM glycine 10% methanol, and 0.1% SDS] (*53*). The membrane was blocked with 5% dried milk, 0.1% Tween 20, and Tris-buffered saline (TBS) [24.8 mM Tris-HCl (pH 7.4), 0.8% NaCl, and 0.02% KCl**]** and incubated with peptide specific antibody against Sec61α (N-terminal peptide, AIKFLEVIKPFC**)**, Sec61*β* (N-terminal peptide, PGPTPSGTNC), TRAM (C-terminal peptide, ADSPRNRKEKSS), TRAPα, or TRAP*δ* in 0.1% Tween 20 and TBS (1:2000 dilution). Antisera against Sec61α and TRAM were kindly provided by K. Matlack. Antisera against Sec61*β* were provided by R. S. Hegde. Antibodies against TRAPα and TRAP*δ* were provided by E. Hartmann. The membrane was washed three times with 0.1% Tween 20 and TBS and then incubated with goat anti-rabbit secondary antibody conjugated with horseradish peroxidase (1:5000 dilution) (Bio-Rad). Bands were detected using the SuperSignal (Pierce, Rockford, IL) reagent on Kodak film (Kodak, Rochester, NY) per the manufacturer's instructions.

## RESULTS

*Identification of Major RAMP Complexes in the ER Membrane by BN-PAGE.* Actively engaged ribosome−translocon complexes (RTCs) were isolated from digitonin-solubilized canine pancreatic ER membranes as diagrammed in Figure 1. Total RAMP proteins were released from pelleted RTCs by puromycin, and solubilized membrane protein complexes were separated from ribosomes by a second centrifugation. Five major bands in the RAMP fraction were easily resolved by BN-PAGE, with sizes of ∼100, ∼115, ∼130, ∼500, and ∼670 kDa (Figure 2A). Mass spectrometry revealed that these major proteins included the Sec61 complex, eukaryotic elongation factor 2 (eEF-2), the TRAP complex, oligosaccharyltransferase (OST or OT), and mitochondrial complex V, respectively. Mitochondrial complex V was often seen as a minor contamination in ER microsome preparations during tissue fractionation. Major complexes such as OST and TRAP were released from RTCs by puromycin under physiological salt conditions (Figure 2A, lane 1), while Sec61 complexes were tightly associated with RTCs, and were only released under high-salt conditions (Figure 2A, lane 2).

*Identification of RAMPs by 2D BN-PAGE/SDS−PAGE.* Components of RAMP complexes isolated by BN-PAGE were then separated in the second dimension by SDS−PAGE and visualized with silver staining (Figure 2B). The subunits of OST, TRAP, TRAM, and Sec61 were identified from excised bands by tandem mass spectrometry (MS/MS) and/or Western blotting analysis. We also identified several additional proteins in the RAMP fraction, which included

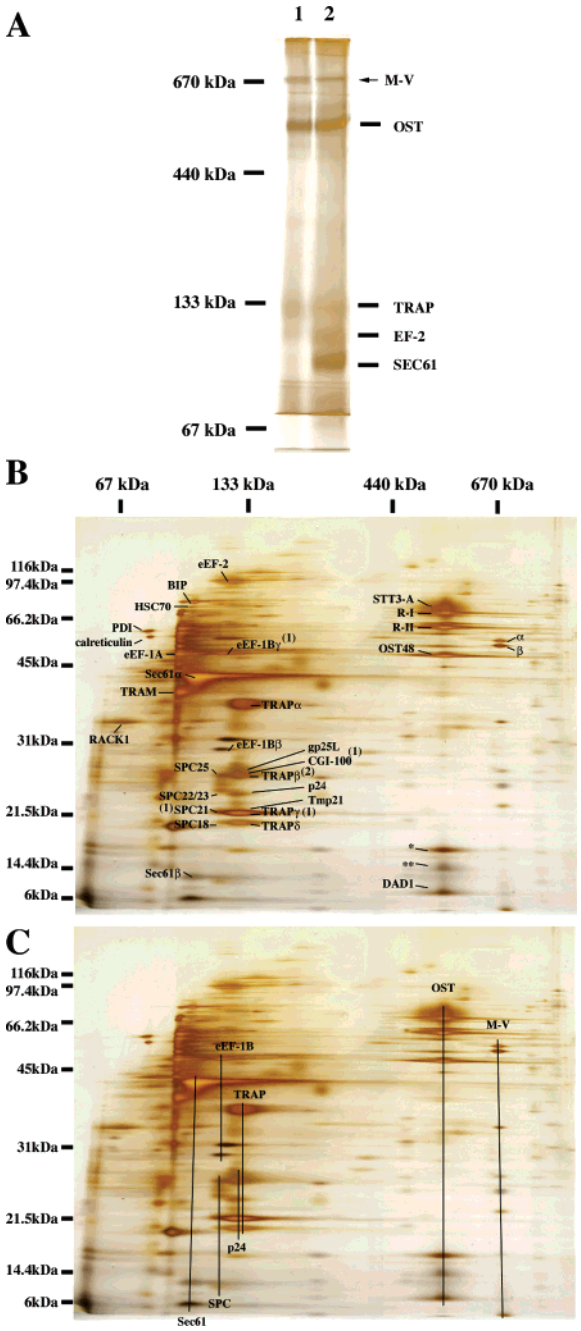


FIGURE 2: BN-PAGE analysis of RAMP proteins. (A) Silver-stained gel showing the RAMP fraction isolated following 2 mM puromycin treatment in the presence of 150 mM NaCl (lane 1) or 1000 mM NaCl (lane 2). The location of ER protein complexes is indicated at the right. M-V is the 670 kDa mitochondrial respiratory chain complex V which is commonly observed as a minor contamination in ER membrane preparations. Molecular markers are indicated. (B) BN-PAGE gel strips were subjected to two-dimensional SDS−PAGE and visualized by silver staining. Spots of interest were excised, digested with trypsin, and subjected to analysis with MS/MS and/or Western blotting. The identities of spots are indicated in panel B and Table 1. Ribophorin I and ribophorin II are abbreviated as R-I and R-II, respectively. The location of molecular markers for the one-dimensional gel is indicated at the top. Molecular markers for the 2D gel are indicated at the left. Note that (1) only one peptide fragment was obtained from this band and (2) TRAP*β* was identified through the analysis tool software, OpenSea. α and *β* indicated proteins were identified as subunits of the mitochondrial complex V (M-V). (C) Migration patterns of individual RAMP complexes are indicated.

four members of the p24 family [gp25L (α subunit), p24

Table 1: Identification of RAMP Proteins and Complexes by 2D BN-PAGE/SDS−PAGE and LC−MS/MS[a]

| complex | protein name | Swiss-Prot entry | NCBI accession no. | MW | peptide ID | sequence coverage |
|---|---|---|---|---|---|---|
| Sec61 | Sec61α[b] | S611_CANFA | 585957 | 52239 | 6 | 13.2 |
| | Sec61β[c] | | | | | |
| TRAP | TRAPα | SSRA_CANFA | 134930 | 31976 | 3 | 20.3 |
| | TRAPβ[d] | SSRB_CANFA | 134931 | 20100 | 5 | 20.2 |
| | TRAPγ[e] | SSRG_HUMAN | 9087205 | 21080 | 1 | 7.6 |
| | TRAPδ | SSRD_HUMAN | 1711550 | 18980 | 2 | 12.1 |
| OST | STT-3A | STT3_MOUSE | 1174470 | 80598 | 8 | 11.5 |
| | ribophorin I | RIB1_HUMAN | 132559 | 68569 | 9 | 15.7 |
| | ribophorin II | RIB2_HUMAN | 9297108 | 69284 | 5 | 7.9 |
| | OST48 | OST4_CANFA | 464319 | 49634 | 7 | 16.6 |
| | KIAA0152 | Y152_HUMAN | 2495712 | 32234 | 3 | 8.6 |
| | DC2 | NP_067050 | 24308271 | 16829 | 2 | 12.8 |
| | KCP2[e] | NP_079603 | 13384696 | 14675 | 1 | 12.5 |
| | DAD1 | DAD1_HUMAN | 4842885 | 12497 | 2 | 19.5 |
| TRAM | TRAM[c] | | | | | |
| SPC | SPC25 | SP25_CANFA | 3183167 | 24942 | 2 | 17.7 |
| | SPC22/23 | SP22_CANFA | 46577647 | 20313 | 2 | 12.8 |
| | SPC21[e] | SPC3_CANFA | 13479 | 21600 | 1 | 4.2 |
| | SPC18 | SPC4_CANFA | 54039633 | 20625 | 2 | 9.5 |
| p24 | gp25L | G25L_CANFA | 120633 | 24882 | 2 | 12.1 |
| | p24 | P24_HUMAN | 3914237 | 22761 | 2 | 13.9 |
| | Tmp21 | TM21_HUMAN | 391589 | 24976 | 2 | 10.5 |
| | CGI-100[e] | CA00_HUMAN | 12585534 | 26005 | 1 | 5.2 |
| chaperones | BIP | GR78_HUMAN | 1491699 | 72333 | 18 | 33.8 |
| | PDI | PDI_HUMAN | 2507460 | 57116 | 8 | 18.7 |
| | calreticulin | CRTC_HUMAN | 117501 | 48142 | 7 | 21.8 |
| | HSC70 | HS7C_HUMAN | 123648 | 70898 | 11 | 28.9 |
| eEF-1A | eEF1A | EF11_HUMAN | 399413 | 50141 | 5 | 12.6 |
| eEF-1B | eEF-1Bβ | EF1B_HUMAN | 119163 | 24764 | 4 | 21.3 |
| | eEF-1Bγ[e] | EF1G_HUMAN | 119165 | 50119 | 1 | 3.0 |
| eEF-2 | eEF-2 | EF2_HUMAN | 119172 | 95338 | 2 | 2.7 |
| miscellaneous | RACK1 | GBLP_HUMAN | 54037168 | 35077 | 7 | 33.1 |

[a] The native RAMP complexes were separated by one-dimensional BN-PAGE, and the associated subunits of the isolated complexes were then separated by 2D SDS−PAGE. Gel bands were excised and analyzed by LC−MS/MS. [b] Identity confirmed by MS/MS and Western blotting. [c] Identity only confirmed by Western blotting. [d] TRAPβ was identified only through the de novo sequencing analysis tool software, OpenSea. [e] Only one peptide fragment was observed.

(β subunit), CGI-100 (γ subunit), and tmp21 (δ subunit)] and four subunits of the signal peptidase complex (SPC) (SPC25, SPC22/23, SPC21, and SPC18). These complexes migrated closely with TRAP at ∼130 kDa on BN-PAGE, consistent with their expected size. Several ER chaperone proteins were also identified, including calreticulin, BIP, HSC70, and PDI, consistent with their expected association with nascent translocating polypeptides. Eukaryotic elongation factors such EF-1A, eEF-1B, and eEF-2 were also present, consistent with their role in translation. These results are summarized in Table 1. In total, six distinct protein complexes and more than 30 nonribosomal proteins were identified in the RAMP fraction (Figure 2C). As expected, these proteins were very highly enriched in ER components known to play a major role in translocation, folding, and cotranslational modification of nascent polypeptides. To our knowledge, these are the first data to show that a (tetrameric) p24 complex is physically associated with engaged RTCs.

*Proteomic Analysis of the OST Complex.* In the current study, we focused on the major OST complex (designated $OSTC_I$) which migrated as a prominent band with an apparent size of ∼500 kDa (Figure 2A). Silver staining of 2D gels revealed the characteristic protein profile expected for mammalian OST (*22*, *31*) (Figure 3). Analysis of these bands by MS/MS verified the identity of all known mammalian OST subunits, STT3-A, ribophorin I, ribophorin II, OST48, and DADI (Table 1 and Figure 3A). Moreover, two additional components of ∼17 and ∼14 kDa copurified with $OSTC_I$ as indicated by single and double asterisks, respectively (Figure 3). $OSTC_I$ isolated from two different ER microsome preparations also identified a slightly smaller (∼470 kDa) complex in addition to the major 500 kDa OST component (compare panels A and B of Figure 3). Notably, the 470 kDa complex was missing the 17 and 14 kDa proteins but retained all essential OST components.

*Differential Release of OST Complexes by Puromycin and High-Salt Treatment.* We next investigated the composition of OST complexes based on their affinity for solubilized RTCs. ER microsomes were solubilized, and RAMPs were sequentially released by puromycin in a stepwise fashion with increasing salt concentrations. This differential RAMP isolation procedure is shown in Figure 1. The solubilized RTCs were washed three times in the 150 mM NaCl buffer to remove loosely associated components prior to puromycin release and high-salt stripping. After each salt wash, the amount of protein released was dramatically decreased (Figure 4, lanes 1−3). Nascent polypeptides were then released with puromycin. This primarily resulted in recovery of TRAPαβγδ and $OSTC_I$ (Figure 4, lane 4, single asterisks). Little release of any RAMPs was observed during subsequent wash steps in the continued presence of puromycin (Figure 4, lane 5). However, re-extraction of these highly purified, puromycin-treated RTCs with high salt (1000 mM NaCl) resulted in the release of several additional post-RAMP complexes, Sec61 (∼100 kDa), and at least two additional bands of ∼600 and ∼700 kDa (Figure 4, lane 6, double asterisks).

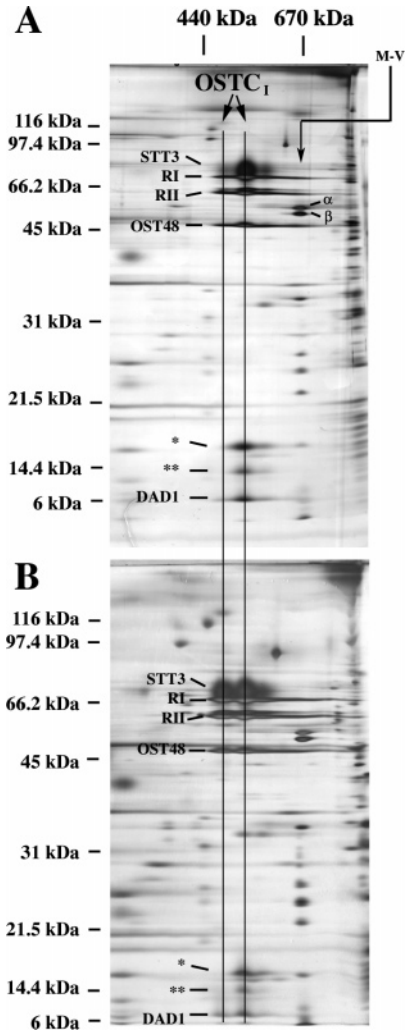


FIGURE 3: Analysis of OST by 2D BN-PAGE/SDS−PAGE. RAMP fractions were isolated from two different preparations of canine ER microsomes (panels A and B) and analyzed as described in the legend of Figure 2. The identity of excised OST subunits is shown. Vertical lines indicate proteins that comprise the major $OSTC_I$ complex migrating at ∼470 and ∼500 kDa in the first dimension on BN-PAGE. The abundance of the 470 kDa species varied significantly between different microsome preparations. The reason for this is unclear. Two novel proteins of ∼17 and ∼14 kDa copurified with the 500 kDa $OSTC_I$ species are denoted with single and double asterisks, respectively. Molecular markers for the one-dimensional BN-PAGE gel are indicated at the top. Locations of α and *β* subunits of the mitochondrial complex V (M-V) are indicated.

*OST Forms Stable Supercomplexes with Sec61 and TRAP Independent of Ribosome Binding.* To determine the composition of OST complexes released under different salt conditions, RAMP and post-RAMP preparations shown in Figure 4 were analyzed by 2D BN-PAGE/SDS−PAGE. Figure 5A shows that puromycin treatment in the presence of 150 mM NaCl released significant amounts of TRAP*αβγδ* and $OSTC_I$. Thus, association of $OSTC_I$ with ribosomes is dependent on the presence of a nascent polypeptide within the ribosome exit tunnel. Cleavage of the peptidyl-tRNA bond and release of polypeptide with puromycin weaken these associations sufficiently such that essentially all $OSTC_I$ is removed from ribosomes at low salt concentrations.

2D BN-PAGE/SDS−PAGE of the post-RAMP fraction identified two additional major complexes of ∼600 and ∼700 kDa that exhibit a higher apparent affinity for ribosomes and were designated $OSTC_{II}$ and $OSTC_{III}$ (Figure 5B). $OSTC_{II}$ contained all previously identified OST subunits and three additional proteins with approximate sizes of 43, 9, and 6 kDa (indicated with carrots). The larger two proteins comigrated with Sec61α and -*β*, and their identities were confirmed by Western blotting analysis (Figure 5C). The largest OST complex ($OSTC_{III}$) migrated at ∼700 kDa and contained all OST subunits, Sec61 components, and four additional proteins of approximately 39, 25, 21, and 18 kDa, which comigrated precisely with TRAP subunits α, *β*, *γ*, and *δ* on SDS−PAGE (indicated with plus signs). Western blotting analysis confirmed the identities of TRAPα and TRAP*δ* in $OSTC_{III}$ (data not shown). Thus, our data indicate that within the actively translating pools of RTCs, there exist subpopulations of OST that can remain associated with Sec61 and TRAP even after release from the ribosome.

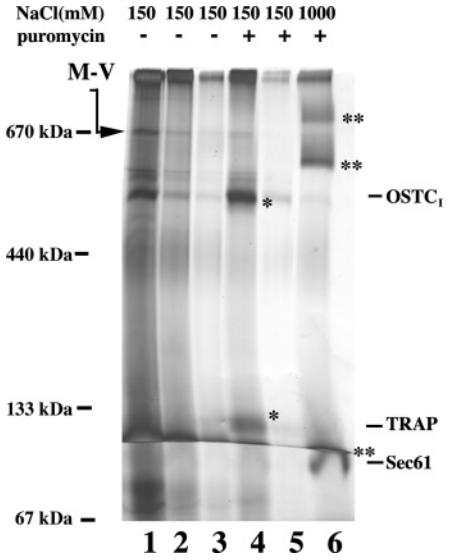


FIGURE 4: BN-PAGE analysis of WASH, RAMP, and post-RAMP fractions. Silver-stained BN-PAGE gel showing WASH, RAMP, and post-RAMP fractions. WASH fractions (lanes 1−3) represent the repeated washing of RTCs prior to puromycin release. Lane 4 contained the RAMP fraction obtained by puromycin treatment. The WASH fraction (lane 5) shows little residual RAMPs following the release of puromycin. Lane 6 contained the post-RAMP fraction obtained by further incubating ribosomes with puromycin and high salt. Single asterisks denote the TRAP (133 kDa) and $OSTC_I$ (500 kDa) complexes that were specifically released in the RAMP fraction (lane 4). Double asterisks denote Sec61 (100 kDa) and three additional complexes (∼600 and ∼700 kDa) which were specifically released in post-RAMP fractions (lane 6).

*Identification of Two Potential Novel Subunits of the OST Complex.* In addition to known subunits, two novel bands of ∼17 and ∼14 kDa copurified with all three OST complexes ($OSTC_I$, $OSTC_{II}$, and $OSTC_{III}$). MS analysis of the 17 kDa protein yielded matches with two predicted trypsin fragments from a 17 kDa protein, human DC2 (GenBank accession no. NP_067050) (12.8% sequence coverage). A search of the TIGR (The Institute of Genomic Research) database of the canine ESTs with the protein sequence of human DC2 revealed two EST sequences, dog|TC4658 and dog|BF228912. Using these ESTs and proteomic data, we deduced the entire canine sequence of DC2 (Figure 6A), which differs from human DC2 by only a single conserved amino acid substitution (Val vs Leu) at residue 25 (an upward arrow, Figure 6A). A domain

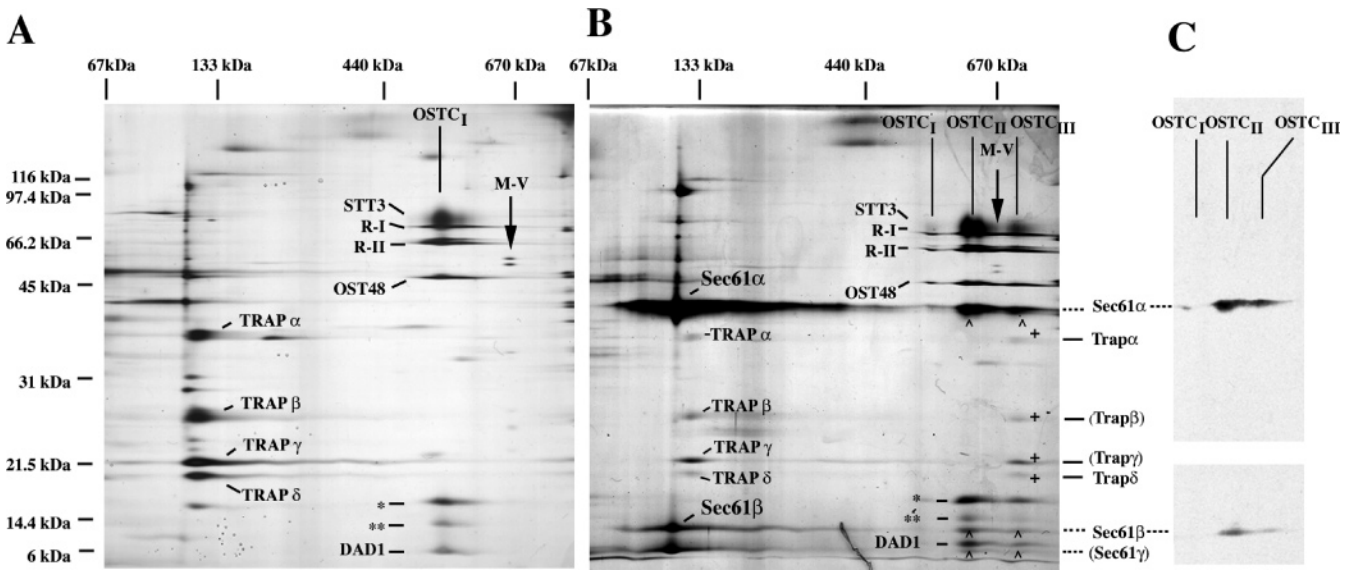


FIGURE 5: Sequential release of OST complexes. RAMP and post-RAMP fractions from Figure 4 were further subjected to 2D SDS−PAGE. (A) RAMP complexes released with puromycin included TRAP and OSTC$_I$. The identity of TRAP and OST subunits is indicated. Two novel proteins of ~17 and ~14 kDa copurified with OST are denoted with single and double asterisks, respectively. (B) High-salt treatment of washed puromycin-treated RTCs released Sec61, OSTC$_{II}$, and OSTC$_{III}$. Carrots indicate 43, 9, and 6 kDa bands that copurified with OSTC$_{II}$ and OSTC$_{III}$ and migrated with Sec61 subunits on 2D SDS−PAGE. The presumptive location of Sec61$\gamma$ is shown in parentheses. (Plus signs indicate 39, 25, 21, and 18 kDa proteins that copurified with OSTC$_{III}$ and migrate with TRAP$\alpha\beta\gamma\delta$ subunits on 2D SDS−PAGE. (C) The presence of Sec61α and Sec61$\beta$ was confirmed as a component of the OSTC$_{II}$ and OSTC$_{III}$ complexes by Western blotting. TRAPα and TRAP$\delta$ were also identified in OSTC$_{III}$ by Western blotting (data not shown). Identities of TRAP$\beta$ and TRAP$\gamma$ are based on locations of these proteins on a 2D SDS−PAGE gel.

architecture search using the Conserved Domain Database (CDD) (Pfam v11.0-7255 PSSMs) found that DC2 is related to the Ost3 and Ost6 family (pfam04756). Sequence alignment (Figure 6A) revealed that DC2 is weakly homologous to the C-terminal halves of yeast Ost3p and Ost6p. The Simple Modular Architecture Research Tool (SMART) and a Kyte−Doolittle hydropathy plot suggested that DC2 contains at least three predicted transmembrane segments which closely resemble three of the four TM segments predicted for yeast Ost3p and Ost6p (Figure 6B). Therefore, DC2 appears to be a distant homologue of yeast Ost3p and Ost6p.

MS/MS analysis of the ~14 kDa OST subunit identified a single fragment (ISSTLYQATAPVLTPAK) that matched a previously described 14 kDa mouse protein, keratinocyte-associated protein 2 (KCP2) (GenBank accession no. NP_079603) (12.5% sequence coverage). Even though only one peptide fragment was identified, this fragment was observed repeatedly in MS analyses from different ER membrane preparations and in different MS facilities. The canine KCP2 homologue was identified from the TIGR canine EST (dog|BQ234307), and the resulting sequences are shown in Figure 7A. The peptide fragment identified from mouse and canine KCP2 has the same peptide mass (ISSTLYQAATPVLTPAK) but differs in sequence by only two residues, 119 (T vs A) and 120 (A vs T). Moreover, analysis of the MS/MS spectrum of the canine peptide fragment unequivocally matched the canine sequence (spectra shown in Figure 7B). KCP2 is highly expressed in pancreas but has no known physiological function (*54*). A search for homologous protein families with the KCP2 protein using BLAST, CDD, and EMBL Harvester did not uncover any homology to known protein families. SMART analysis and a Kyte−Doolittle hydropathy plot predicted that KCP2 contains four transmembrane segments (Figure 7C). KCP2 also has a KKXX sequence motif at its C-terminus, suggesting that it may be an ER-localized membrane protein.

## DISCUSSION

*BN-PAGE Identified Multiple OST Complexes in the RAMP Fraction.* In our study, we have characterized the subunit composition of RAMP complexes derived from mammalian ER membranes. We utilized BN-PAGE which separates solubilized membrane protein complexes under native conditions utilizing Coomassie G250 dyes as negative charge carriers. This approach minimizes undesirable hydrophobic interaction, aggregation, and precipitation and allows large membrane complexes to be separated in a single step by gel electrophoresis (*34*, *35*). Digitonin was used to solubilize microsomes because it maintains the integrity of ribosome−translocon complexes (RTCs) (*29*, *30*, *55*), and it has been successfully used for purification of intact OST (*7*, *20*, *22*). In contrast, other detergents such as Triton X-100 and diheptanoyl-*sn*-phosphatidylcholine (DHPC) disrupt the ribosome−translocon junction (refs *31* and *55* and data not shown). As expected, BN-PAGE identified all known major RAMP proteins from actively engaged ribosome−translocon (RTC) complexes on the basis of their selective release by puromycin (*31*). In combination with MS/MS, we identified more than 30 nonribosomal, RAMP proteins and six distinct RAMP complexes that include Sec61, SPC, p24, TRAP, TRAM, and OST. Thus, this technique provides a powerful tool for studying ER membrane proteins because intact complexes can be separated with significant precision in the first dimension on the basis of overall size, and subunits can be readily separated, visualized, and identified in the second dimension. Our observation that SPC associates with RTCs is consistent with findings that SPC25 cross-links to Sec61$\beta$ (*56*) and further indicates that the entire SPC complex maintains its association with the RTC after solubilization

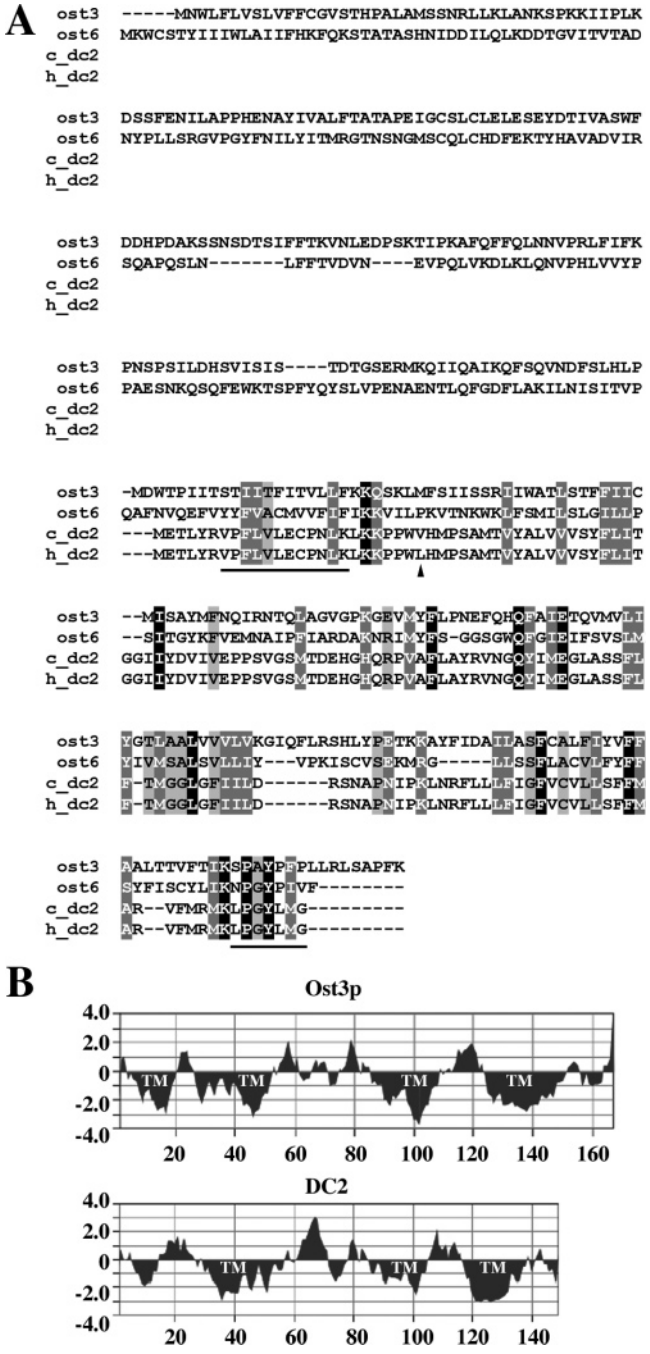


FIGURE 6: Identification of the human and canine DC2 as an Ost3p and Ost6p homologue. (A) Peptide fragments identified through MS/MS are indicated with solid lines. The arrowhead indicates the single difference between the human and canine DC2 sequences. Human and canine sequences were aligned with yeast Ost3p and Ost6p using the web-based Clustal W. Identical amino acids in human, canine DC2, and yeast Ost3p/Ost6p sequences are indicated as white letters on a black background. Highly conserved amino acids are indicated as white letters on a dark gray background. Relatively conserved amino acids are indicated as black letters on a light gray background. c_dc2 and h_dc2 indicate canine DC2 and human DC2, respectively. (B) Hydropathy analyses of canine DC2 and the C-terminal half of yeast Ost3p were generated by the Kyte−Doolittle hydropathy plot (*52*). Predicted transmembrane segments are shown.

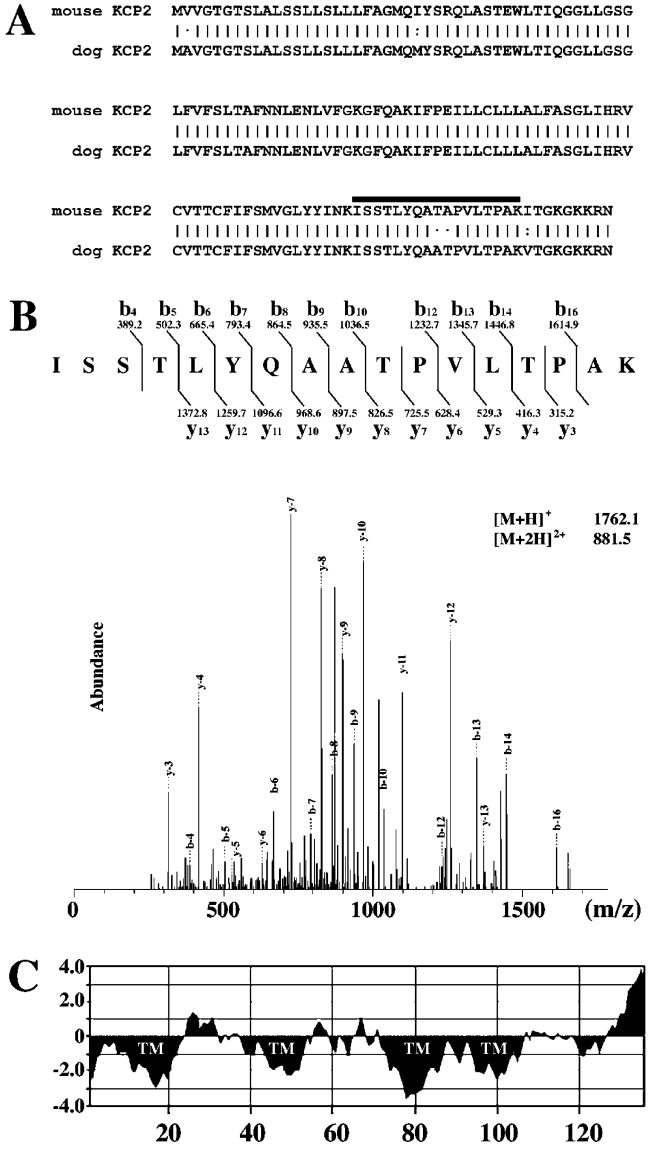


FIGURE 7: MS/MS identification of KCP2. (A) The peptide fragment identified via mass spectrometry is indicated by the solid line. The identified canine sequence was aligned with murine KCP2 using the web-based Clustal W. The identical amino acids are indicated as solid lines, and highly conserved amino acids are indicated as two dots. Relatively conserved amino acids are indicated as single dots. (B) MS/MS spectrum of the identified KCP2 peptide. The spectra for C-terminal (y ions) and N-terminal (b ions) fragments were exceedingly well matched with the spectrum for ISSTLYQAATPVLTPAK. The average masses of singly and doubly charged parent ions are given in the top right corner of the spectra. (C) Hydropathy analysis of canine KCP2 was generated by the Kyte−Doolittle hydropathy plot (*52*). Predicted transmembrane segments are shown.

with digitonin. Members of the p24 family are putative ER cargo receptors, which are known to be localized at ER exit sites and in the intermediate and cis-Golgi compartments of the early secretory pathway (*57*−*59*). Identification of tetrameric p24 in the RAMP fraction was therefore surprising and raises the possibility that its association with ER cargo proteins may be initiated at early stages of translation.

*OST Forms Multiple Complexes in Native ER Membranes that Vary in Composition and Ribosome Affinity*. The presence of multiple OST complexes was reported previously in canine pancreatic microsomes. Kelleher et al. demonstrated that at least three OST complexes are present with different STT3 subunits and enzymatic activities (*20*). Wang and Dobberstein also observed two different OST complexes (480 and 450 kDa), one of which contained 33 and 10 kDa subunits. In our study, BN-PAGE provided sufficient resolu-

tion for clear identification of three distinct OST complexes that were remarkably stable in the detergent solution (more than 48 h) and which were distinguished by their molecular size, ribosome binding, puromycin and salt sensitivity, and affinities for different translocon components. $OSTC_I$ was released by puromycin treatment of solubilized RTCs under physiological salt conditions and contained the essential OST subunits (STT3-A, ribophorin I, ribophorin II, OST48, and DAD1) as well as two additional 17 and 14 kDa proteins. Because $OSTC_I$ was quantitatively released by puromycin, we conclude that it is derived from actively engaged RTCs and that its affinity for the RTC is directly affected by the presence of the nascent polypeptide. This suggests that the major functional form of OST in mammalian pancreatic ER membranes consists of at least seven subunits identified in this study.

In contrast, a very different pattern was observed when puromycin-treated RTCs were further incubated under high-salt conditions. In addition to the release of Sec61, at least two additional complexes were visible in the first dimension by BN-PAGE (Figure 4, lane 6). $OSTC_I$ represented a very minor component of these post-RAMP fractions, whereas $OSTC_{II}$ (~600 kDa) and $OSTC_{III}$ (~700 kDa) were prominent. These complexes were quantitatively released with high-salt treatment even after multiple low-salt washes, demonstrating that they represent distinct populations of OST with different binding affinity for the RTC and not simply residual puromycin-sensitive complexes. Consistent with their increased size, $OSTC_{II}$ and $OSTC_{III}$ contained several additional proteins that included components of heterotrimeric Sec61$\alpha\beta\gamma$ and tetrameric TRAP$\alpha\beta\gamma\delta$ complexes (Figure 5B). Thus, OST can form stable complexes with TRAP and Sec61 even after being released from the ribosome. Moreover, two novel 17 and 14 kDa proteins copurified with all three OST complexes ($OSTC_I$, $OSTC_{II}$, and $OSTC_{III}$), suggesting that they represent actual OST subunits and not a comigrating contaminant of $OSTC_I$.

*Two Potential New Subunits of the Mammalian OST Complex.* MS/MS analysis of the 17 kDa band identified two peptides whose fragmentation pattern matched those predicted from human DC2 (12.8% sequence coverage), a 149-amino acid protein of unknown function. We identified the canine ortholog from a BLAST search against the TIGR dog EST database. A search for homologous conserved domains in DC2 using CDD in NCBI and alignment algorithms using MultAlin (*60*) and Clustal W (http://www.ebi.ac.uk/clustalw) revealed that DC2 is weakly homologous to the C-terminal half of yeast Ost3p and Ost6p. Because DC2 copurified with all OST complexes, we propose that DC2 is a component of the mammalian OST complex. It is interesting that Ost3p and Ost6p are not required in yeast, but deletion leads to selective underglycosylation of certain glycoprotein substrates (*16*, *17*). If DC2 provides the equivalent Ost3p and Ost6p functions in mammalian OST, it is conceivable that it might also modulate nascent polypeptide glycosylation. Recent studies suggest that the N-terminal half of Ost3p and Ost6p contains oxidoreductase activity (*24*). This domain is notably missing from DC2, suggesting either that this activity is not required for mammalian OST function or that it is provided by a different subunit. In this regard, sequence analysis identified two 33 kDa mammalian proteins, N33 and IAP, that are weakly homologous to Ost3p and Ost6p and may also funtion as oxidoreductases (*17*, *20*, *24*). Neither N33 nor IAP has been formally shown to associate with purified mammalian OST from pancreatic microsomes despite a high level of (IAP) pancreatic expression (*20*). However, Nilsson et al. reported as unpublished data that N33 and IAP could assemble into the OST complex when expressed in mammalian cells (*28*). While our 2D BN-PAGE/SDS−PAGE analyses failed to identify N33 or IAP, it remains possible that these proteins associate with OST in a manner that is sensitive to the solubilization and/or isolation procedures used here. Further study is therefore needed to confirm the role of N33 and/or IAP in mammalian OST function.

MS/MS also tentatively identified a second prominent 14 kDa protein that copurified with $OSTC_I$, $OSTC_{II}$, and $OSTC_{III}$ complexes as murine "keratinocyte-associated protein 2" (KCP2). Canine KCP2 was deduced from an EST from the TIGR dog EST database. The calculated molecular mass of KCP2 matches its molecular size as determined by SDS−PAGE (14 kDa). SMART analysis predicted that KCP2 contains four transmembrane domains and a C-terminal ER localization KKXX motif (*61*). Moreover, Northern blot analysis on tissue distribution has previously shown that KCP2 is highly expressed in pancreas (*54*). BLAST, CDD, and Harvester searches (http://harvester.embl.de/) did not identify related proteins among known protein families, and the function of KCP2 remains unknown. Because only a single peptide was detected by MS/MS and it is not homologous to any OST subunits, further study is required to definitively determine the function of KCP2 and its relevance to OST.

## SUMMARY

The presence of multiple OST complexes in native ER membranes implies that OST interactions with actively engaged RTCs are pleiotropic and that OST can be an integral component of the ER translocation machinery. A significant proportion of OST is readily released from RTCs in the absence of a nascent polypeptide chain, whereas a subset of OST remains tightly bound, presumably via interactions with Sec61 and/or TRAP. It is interesting that $OSTC_{II}$ and $OSTC_{III}$ are stripped from the RTC under the same conditions required to remove Sec61, whereas the majority of TRAP was released from RTCs following puromycin treatment under low-salt conditions (Figure 5A). Only a small fraction of Sec61 and TRAP in the ER membrane (<10%) was recovered in the $OSTC_{II}$ and $OSTC_{III}$ complexes. Thus, these complexes represent either a very minor fraction of engaged RTCs or a transient state of OST that is effectively captured at a particular stage of its functional cycle. In this regard, ER microsomes used here were isolated from canine pancreas that presumably contain a wide variety of native protein substrates at random stages of translocation. Because glycosylation consensus sites can exist virtually anywhere, OST must continuously scan the nascent polypeptide as it exits the translocon and translocates into the ER lumen (*62*). Therefore, one possibility is that OST interactions with translocon components might be influenced by the nature of the substrate. Consistent with this notion, recent studies indicate that ribophorin I can remain associated with some nascent polypeptides even after puromycin release and raise the possibility that ribophorin I

might function to hold certain substrates in the proximity of the active site of oligosaccharyltransferase (*63*). It is also possible that the process of scanning the translocating nascent polypeptide or active engagement of glycosylation sites might alter the relationship between OST, the translocon, and/or the ribosome. Finally, different classes of signal sequences appear to regulate early formation of the ribosome−translocon junction via selective use of translocation-associated proteins (i.e., TRAM and TRAP) (*64*). Thus, the affinity of OST for Sec61 and TRAP might reflect a broader reorganization of translocon structure. While we cannot yet distinguish which of these possibilities best explains our data, it is clear that OST is capable of directly interacting in a stable manner with the translocon and its accessory components. These highly pleiotropic interactions could provide a means of controlling N-linked glycosylation during translation and translocation of the nascent polypeptide.

## ACKNOWLEDGMENT

We thank Dr. George M. Hilliard of the University of Tennessee Health Science Center (Memphis, TN) for assistance with mass spectrometry analysis and Drs. Kent Matlack, Ramanujan S. Hegde, and Enno Hartmann for generously providing Sec61α, Sec61*β*, and TRAPα and TRAP*δ* antibodies, respectively. We also thank Dr. Sri Nagalla for access to the OpenSea program and members of the Skach lab for valuable advice and comments.

## REFERENCES

1. Kornfeld, R., and Kornfeld, S. (1985) Assembly of asparagine-linked oligosaccharides, *Annu. Rev. Biochem. 54*, 631−664.
2. Ou, W. J., Cameron, P. H., Thomas, D. Y., and Bergeron, J. J. (1993) Association of folding intermediates of glycoproteins with calnexin during protein maturation, *Nature 364*, 771−776.
3. Helenius, A., and Aebi, M. (2004) Roles of N-linked glycans in the endoplasmic reticulum, *Annu. Rev. Biochem. 73*, 1019−1049.
4. Molinari, M., and Helenius, A. (1999) Glycoproteins form mixed disulphides with oxidoreductases during folding in living cells, *Nature 402*, 90−93.
5. Knauer, R., and Lehle, L. (1994) The N-oligosaccharyltransferase complex from yeast, *FEBS Lett. 344*, 83−86.
6. Yan, Q., and Lennarz, W. J. (1999) Oligosaccharyltransferase: A complex multisubunit enzyme of the endoplasmic reticulum, *Biochem. Biophys. Res. Commun. 266*, 684−689.
7. Kelleher, D. J., Kreibich, G., and Gilmore, R. (1992) Oligosaccharyltransferase activity is associated with a protein complex composed of ribophorins I and II and a 48 kd protein, *Cell 69*, 55−65.
8. Silberstein, S., and Gilmore, R. (1996) Biochemistry, molecular biology, and genetics of the oligosaccharyltransferase, *FASEB J. 10*, 849−858.
9. Dempski, R. E., Jr., and Imperiali, B. (2002) Oligosaccharyl transferase: Gatekeeper to the secretory pathway, *Curr. Opin. Chem. Biol. 6*, 844−850.
10. Spirig, U., Glavas, M., Bodmer, D., Reiss, G., Burda, P., Lippuner, V., te Heesen, S., and Aebi, M. (1997) The STT3 protein is a component of the yeast oligosaccharyltransferase complex, *Mol. Gen. Genet. 256*, 628−637.
11. Karaoglu, D., Kelleher, D. J., and Gilmore, R. (1997) The highly conserved Stt3 protein is a subunit of the yeast oligosaccharyltransferase and forms a subcomplex with Ost3p and Ost4p, *J. Biol. Chem. 272*, 32513−32520.
12. te Heesen, S., Knauer, R., Lehle, L., and Aebi, M. (1993) Yeast Wbp1p and Swp1p form a protein complex essential for oligosaccharyl transferase activity, *EMBO J. 12*, 279−284.
13. Silberstein, S., Collins, P. G., Kelleher, D. J., Rapiejko, P. J., and Gilmore, R. (1995) The α subunit of the *Saccharomyces cerevisiae* oligosaccharyltransferase complex is essential for vegetative growth of yeast and is homologous to mammalian ribophorin I, *J. Cell Biol. 128*, 525−536.
14. Pathak, R., Parker, C. S., and Imperiali, B. (1995) The essential yeast NLT1 gene encodes the 64 kDa glycoprotein subunit of the oligosaccharyl transferase, *FEBS Lett. 362*, 229−234.
15. Silberstein, S., Collins, P. G., Kelleher, D. J., and Gilmore, R. (1995) The essential OST2 gene encodes the 16-kD subunit of the yeast oligosaccharyltransferase, a highly conserved protein expressed in diverse eukaryotic organisms, *J. Cell Biol. 131*, 371−383.
16. Karaoglu, D., Kelleher, D. J., and Gilmore, R. (1995) Functional characterization of Ost3p. Loss of the 34-kD subunit of the *Saccharomyces cerevisiae* oligosaccharyltransferase results in biased underglycosylation of acceptor substrates, *J. Cell Biol. 130*, 567−577.
17. Knauer, R., and Lehle, L. (1999) The oligosaccharyltransferase complex from *Saccharomyces cerevisiae*. Isolation of the OST6 gene, its synthetic interaction with OST3, and analysis of the native complex, *J. Biol. Chem. 274*, 17249−17256.
18. Chi, J. H., Roos, J., and Dean, N. (1996) The OST4 gene of *Saccharomyces cerevisiae* encodes an unusually small protein required for normal levels of oligosaccharyltransferase activity, *J. Biol. Chem. 271*, 3132−3140.
19. Reiss, G., te Heesen, S., Gilmore, R., Zufferey, R., and Aebi, M. (1997) A specific screen for oligosaccharyltransferase mutations identifies the 9 kDa OST5 protein required for optimal activity in vivo and in vitro, *EMBO J. 16*, 1164−1172.
20. Kelleher, D. J., Karaoglu, D., Mandon, E. C., and Gilmore, R. (2003) Oligosaccharyltransferase isoforms that contain different catalytic STT3 subunits have distinct enzymatic properties, *Mol. Cell 12*, 101−111.
21. Silberstein, S., Kelleher, D. J., and Gilmore, R. (1992) The 48-kDa subunit of the mammalian oligosaccharyltransferase complex is homologous to the essential yeast protein WBP1, *J. Biol. Chem. 267*, 23658−23663.
22. Kelleher, D. J., and Gilmore, R. (1997) DAD1, the defender against apoptotic cell death, is a subunit of the mammalian oligosaccharyltransferase, *Proc. Natl. Acad. Sci. U.S.A. 94*, 4994−4999.
23. Zubkov, S., Lennarz, W. J., and Mohanty, S. (2004) Structural basis for the function of a minimembrane protein subunit of yeast oligosaccharyltransferase, *Proc. Natl. Acad. Sci. U.S.A. 101*, 3821−3826.
24. Fetrow, J. S., Siew, N., Di Gennaro, J. A., Martinez-Yamout, M., Dyson, H. J., and Skolnick, J. (2001) Genomic-scale comparison of sequence- and structure-based methods of function prediction: Does structure provide additional insight? *Protein Sci. 10*, 1005−1014.
25. Helenius, A. (1994) How N-linked oligosaccharides affect glycoprotein folding in the endoplasmic reticulum, *Mol. Biol. Cell 5*, 253−265.
26. Popov, M., Tam, L. Y., Li, J., and Reithmeier, R. A. (1997) Mapping the ends of transmembrane segments in a polytopic membrane protein. Scanning N-glycosylation mutagenesis of extracytosolic loops in the anion exchanger, band 3, *J. Biol. Chem. 272*, 18325−18332.
27. Nilsson, I. M., and von Heijne, G. (1993) Determination of the distance between the oligosaccharyltransferase active site and the endoplasmic reticulum membrane, *J. Biol. Chem. 268*, 5798−5801.
28. Nilsson, I., Kelleher, D. J., Miao, Y., Shao, Y., Kreibich, G., Gilmore, R., von Heijne, G., and Johnson, A. E. (2003) Photocross-linking of nascent chains to the STT3 subunit of the oligosaccharyltransferase complex, *J. Cell Biol. 161*, 715−725.
29. Görlich, D., Prehn, S., Hartmann, E., Kalies, K. U., and Rapoport, T. A. (1992) A mammalian homolog of SEC61p and SECYp is associated with ribosomes and nascent polypeptides during translocation, *Cell 71*, 489−503.
30. Menetret, J. F., Neuhof, A., Morgan, D. G., Plath, K., Radermacher, M., Rapoport, T. A., and Akey, C. W. (2000) The structure of ribosome-channel complexes engaged in protein translocation, *Mol. Cell 6*, 1219−1232.
31. Wang, L., and Dobberstein, B. (1999) Oligomeric complexes involved in translocation of proteins across the membrane of the endoplasmic reticulum, *FEBS Lett. 457*, 316−322.
32. Hartmann, E., Görlich, D., Kostka, S., Otto, A., Kraft, R., Knespel, S., Burger, E., Rapoport, T. A., and Prehn, S. (1993) A tetrameric complex of membrane proteins in the endoplasmic reticulum, *Eur. J. Biochem. 214*, 375−381.
33. Snapp, E. L., Reinhart, G. A., Bogert, B. A., Lippincott-Schwartz, J., and Hegde, R. S. (2004) The organization of engaged and

quiescent translocons in the endoplasmic reticulum of mammalian cells, *J. Cell Biol. 164*, 997−1007.
34. Schägger, H., and von Jagow, G. (1991) Blue native electrophoresis for isolation of membrane protein complexes in enzymatically active form, *Anal. Biochem. 199*, 223−231.
35. Schägger, H., Cramer, W. A., and von Jagow, G. (1994) Analysis of molecular masses and oligomeric states of protein complexes by blue native electrophoresis and isolation of membrane protein complexes by two-dimensional native electrophoresis, *Anal. Biochem. 217*, 220−230.
36. Walter, P., and Blobel, G. (1983) Preparation of microsomal membranes for cotranslational protein translocation, *Methods Enzymol. 96*, 84−93.
37. Oberdorf, J., and Skach, W. R. (2002) In vitro reconstitution of CFTR biogenesis and degradation, *Methods Mol. Med. 70*, 295−310.
38. Laemmli, U. K. (1970) Cleavage of structural proteins during the assembly of the head of bacteriophage T4, *Nature 227*, 680−685.
39. Blum, H., Beier, H., and Gross, H. J. (1987) Imporved silver staining of plant proteins, RNA, and DNA in polyacrylamide gels, *Electrophoresis 8*, 93−99.
40. Moertz, E., Krogh, T. N., Henrik, V. K., and Gorg, A. (2004) Improved silver staining protocols compatible with large-scale protein identification, http://www.bioc.cam.ac.uk/pnac/Poster-Silverstain.pdf.
41. Courchesne, P. L., and Patterson, S. D. (1999) Identification of proteins by matrix-assisted laser desorption/ionization mass spectrometry using peptide and fragment ion masses, *Methods Mol. Biol. 112*, 487−511.
42. Wang-Su, S. T., McCormack, A. L., Yang, S., Hosler, M. R., Mixon, A., Riviere, M. A., Wilmarth, P. A., Andley, U. P., Garland, D., Li, H., David, L. L., and Wagner, B. J. (2003) Proteome analysis of lens epithelia, fibers, and the HLE B-3 cell line, *Invest. Ophthalmol. Visual Sci. 44*, 4829−4836.
43. Eng, J. K., McCormack, A. L., and Yates, J. R., III (1994) An Approach to Correlate Tandem Mass Spectral Data of Peptides with Amino Acid Sequences in a Protein Database, *J. Am. Soc. Mass Spectrom. 5*, 976−989.
44. Tabb, D. L., McDonald, W. H., and Yates, J. R., III (2002) DTASelect and Contrast: Tools for assembling and comparing protein identifications from shotgun proteomics, *J. Proteome Res. 1*, 21−26.
45. Taylor, J. A., and Johnson, R. S. (2001) Implementation and uses of automated de novo peptide sequencing by tandem mass spectrometry, *Anal. Chem. 73*, 2594−2604.
46. Searle, B. C., Dasari, S., Turner, M., Reddy, A. P., Choi, D., Wilmarth, P. A., McCormack, A. L., David, L. L., and Nagalla, S. R. (2004) High-throughput identification of proteins and unanticipated sequence modifications using a mass-based alignment algorithm for MS/MS de novo sequencing results, *Anal. Chem. 76*, 2220−2230.
47. Searle, B. C., Dasari, S., Wilmarth, P. A., Reddy, A. P., David, L. L., and Nagalla, S. R. (2005) Identification of protein modifications using the OpenSea alignment algorithm, *J. Proteome Res.* (in press).
48. Altschul, S. F., Madden, T. L., Schaffer, A. A., Zhang, J., Zhang, Z., Miller, W., and Lipman, D. J. (1997) Gapped BLAST and PSI-BLAST: A new generation of protein database search programs, *Nucleic Acids Res. 25*, 3389−3402.
49. Marchler-Bauer, A., Anderson, J. B., DeWeese-Scott, C., Fedorova, N. D., Geer, L. Y., He, S., Hurwitz, D. I., Jackson, J. D., Jacobs, A. R., Lanczycki, C. J., Liebert, C. A., Liu, C., Madej, T., Marchler, G. H., Mazumder, R., Nikolskaya, A. N., Panchenko, A. R., Rao, B. S., Shoemaker, B. A., Simonyan, V., Song, J. S., Thiessen, P. A., Vasudevan, S., Wang, Y., Yamashita, R. A., Yin, J. J., and Bryant, S. H. (2003) CDD: A curated Entrez database of conserved domain alignments, *Nucleic Acids Res. 31*, 383−387.
50. Letunic, I., Copley, R. R., Schmidt, S., Ciccarelli, F. D., Doerks, T., Schultz, J., Ponting, C. P., and Bork, P. (2004) SMART 4.0: Towards genomic data integration, *Nucleic Acids Res. 32* (Database Issue), D142−D144.
51. Schultz, J., Milpetz, F., Bork, P., and Ponting, C. P. (1998) SMART, a simple modular architecture research tool: Identification of signaling domains, *Proc. Natl. Acad. Sci. U.S.A. 95*, 5857−5864.
52. Kyte, J., and Doolittle, R. F. (1982) A simple method for displaying the hydropathic character of a protein, *J. Mol. Biol. 157*, 105−132.
53. Towbin, H., Staehelin, T., and Gordon, J. (1979) Electrophoretic transfer of proteins from polyacrylamide gels to nitrocellulose sheets: Procedure and some applications, *Proc. Natl. Acad. Sci. U.S.A. 76*, 4350−4354.
54. Bonkobara, M., Das, A., Takao, J., Cruz, P. D., and Ariizumi, K. (2003) Identification of novel genes for secreted and membrane-anchored proteins in human keratinocytes, *Br. J. Dermatol. 148*, 654−664.
55. Potter, M. D., and Nicchitta, C. V. (2002) Endoplasmic reticulum-bound ribosomes reside in stable association with the translocon following termination of protein synthesis, *J. Biol. Chem. 277*, 23314−23320.
56. Kalies, K. U., Rapoport, T. A., and Hartmann, E. (1998) The $\beta$ subunit of the Sec61 complex facilitates cotranslational protein transport and interacts with the signal peptidase during translocation, *J. Cell Biol. 141*, 887−894.
57. Blum, R., Feick, P., Puype, M., Vandekerckhove, J., Klengel, R., Nastainczyk, W., and Schulz, I. (1996) Tmp21 and p24A, two type I proteins enriched in pancreatic microsomal membranes, are members of a protein family involved in vesicular trafficking, *J. Biol. Chem. 271*, 17183−17189.
58. Marzioch, M., Henthorn, D. C., Herrmann, J. M., Wilson, R., Thomas, D. Y., Bergeron, J. J., Solari, R. C., and Rowley, A. (1999) Erp1p and Erp2p, partners for Emp24p and Erv25p in a yeast p24 complex, *Mol. Biol. Cell 10*, 1923−1938.
59. Kuiper, R. P., Bouw, G., Janssen, K. P., Rotter, J., van Herp, F., and Martens, G. J. (2001) Localization of p24 putative cargo receptors in the early secretory pathway depends on the biosynthetic activity of the cell, *Biochem. J. 360*, 421−429.
60. Corpet, F. (1988) Multiple sequence alignment with hierarchical clustering, *Nucleic Acids Res. 16*, 10881−10890.
61. Townsley, F. M., and Pelham, H. R. (1994) The KKXX signal mediates retrieval of membrane proteins from the Golgi to the ER in yeast, *Eur. J. Cell Biol. 64*, 211−216.
62. Johnson, A. E., and van Waes, M. A. (1999) The translocon: A dynamic gateway at the ER membrane, *Annu. Rev. Cell Dev. Biol. 15*, 799−842.
63. Wilson, C. M., Kraft, C., Duggan, C., Ismail, N., Crawshaw, S. G., and High, S. (2005) Ribophorin I associates with a subset of membrane proteins after their integration at the sec61 translocon, *J. Biol. Chem. 280*, 4195−4206.
64. Fons, R. D., Bogert, B. A., and Hegde, R. S. (2003) Substrate-specific function of the translocon-associated protein complex during translocation across the ER membrane, *J. Cell Biol. 160*, 529−539.

BI047328F